Bioactive Materials 3 (2018) 157–166

Contents lists available at ScienceDirect

Bioactive Materials

journal homepage: http://www.keaipublishing.com/en/journals/bioactive-materials/

Studies on the cytocompatibility, mechanical and antimicrobial properties of 3D printed poly(methyl methacrylate) beads

David K. Mills [a, b, *], Uday Jammalamadaka [a], Karthik Tappa [a], Jeffery Weisman [a]

[a] Center for Biomedical Engineering and Rehabilitation Science, USA
[b] The School of Biological Sciences, Louisiana Tech University, Ruston, LA 71272, USA

ARTICLE INFO

Article history:
Received 13 December 2017
Received in revised form
26 January 2018
Accepted 27 January 2018
Available online 13 February 2018

Keywords:
3D printing
Antibacterials
Drug delivery
Halloysite nanotubes
Medical devices
Nanotechnology

ABSTRACT

Osteomyelitis is typically a bacterial infection (usually from Staphylococcus) or, more rarely, a fungal infection of the bone. It can occur in any bone in the body, but it most often affects the long bones (leg and arm), vertebral (spine), and bones of the foot. Microbial success in osteomyelitis is due to their ability to form biofilms which inhibit the wound healing process and increases resistance to anti-infective agents. Also, biofilms do not allow easy penetration of antibiotics into their matrix making clinical treatment a challenge. The development of local antibiotic delivery systems that deliver high concentrations of antibiotics to the affected site is an emerging area of research with great potential. Standard treatment includes antibiotic therapy, either locally or systemically and refractory cases of osteomyelitis may lead to surgical intervention and a prolonged course of antibiotic treatment involving placement of antibiotic-doped beads or spacers within the wound site. There are disadvantages with this treatment modality including insufficient mixing of the antibiotic, lack of uniform bead size, resulting in lower antibiotic availability, and limitations on the antibiotics employed. Thus, a method is needed to address biofilm formations in the wound and on the surface of the surgical implants to prevent osteomyelitis. In this study, we show that all antibiotics studied were successfully doped into PMMA and antibiotic-doped 3D printed beads, disks, and filaments were easily printed. The growth inhibition capacity of the antibiotic-loaded PMMA 3D printed constructs was also demonstrated.

1. Introduction

Osteomyelitis is a difficult-to-treat infectious disease that affects the young and the elderly [1,2]. Treatment of osteomyelitis has improved substantially over the years. However response to treatments vary considerably depending upon the mechanism of infection, its virulence, patient response to treatment, and the nature of the microbial pathogen causing the infection [3–5]. Chronic osteomyelitis requires surgical debridement and high dose antibiotic treatment, given either locally or systemically, for up to six weeks in cases of chronic osteomyelitis [1,4–6]. The selection of an antibiotic regimen in a patient is dependent on many different factors including the causative organism, co-morbidities, severity of the disease, pharmacological cost and concern over antibiotic resistance [1,6,7].

With systemic administration, penetration of the antibiotic into the affected bone is uneven and in some cases, is not effective [7], and the use of high dose concentration can cause other complications [2,6]. Systemic delivery of antibiotics affects the intended site as well as unaffected tissues, and for some patients, raises the risks of cytotoxicity, nephrotoxicity and the potential for an increase in antibiotic resistance [6]. It is clinically advantageous to have treatment without unnecessary and harmful side effects. Local delivery of antibiotics in the management of chronic osteomyelitis has the advantage of delivering high antibiotic concentrations at the site of infection without the systemic toxicity associated with the parenteral route [6,8–10]. The most commonly used non-biodegradable carrier material has been antibiotic-loaded bone cement poly(-methyl methacrylate) (PMMA) in the form of antibiotic-doped beads, nails, spacers or bone cement [11–14]. The constructs can provide high concentrations of broad-spectrum antibiotics to the most critical sites of infection; areas that cannot be reached by

* Corresponding author. Center for Biomedical Engineering and Rehabilitation Science, Louisiana Tech University, Ruston, LA 71272, USA.
E-mail address: dkmills@latech.edu (D.K. Mills).
Peer review under responsibility of KeAi Communications Co., Ltd.

https://doi.org/10.1016/j.bioactmat.2018.01.006

systemically delivered antibiotics [8,15]. There are, however, some disadvantages or concerns about the use of antibiotic-loaded PMMA including the high exothermic temperatures generated in PMMA polymerization, limitations on the types of antibiotics that may be employed, uneven antibiotic release rates, and the need for a second surgery to remove the PMMA [15,16].

In response, the use of bioabsorbable or biodegradable material has been developed in recent years that combine the local delivery of antibiotics in biodegradable and osteogenic materials [8,15,16]. These systems have been shown to be promising alternatives for the treatment of osteomyelitis because they can produce bactericidal concentrations for extended periods of time and without the toxicity associated with other delivery systems. Silicate-based systems [16] and bioglasses [17] have been studied for the treatment of chronic osteomyelitis. The local delivery systems that have shown the most promise include osteoconductive bioceramics (calcium sulfate, tricalcium phosphate or hydroxyapatite) or bioceramic composites infused with antimicrobial agents [18–21]. The key advantage of these systems is they bond strongly with bone, act as a void filler, and will convert to a type of hydroxyapatite and promote osteogenesis at the defect site [22,23]. Despite the accepted use of local antibiotic therapy, robust clinical data regarding Indications for use, optimum dosages, types of antibiotics, elution properties and pharmacokinetics are still poorly defined [16]. However, there is a consensus view that a therapy that provides high local drug concentrations for a sustained period is highly desired [6,8,15].

The key features of 3D printing (accuracy, speed, tunability) offer the potential for on-demand, customized, and patient-specific antibiotic treatments, and possibly a technology that can address the disadvantages with current antibiotic carrier systems. It has the potential to provide high concentrations of antibiotics delivered locally and without the harmful side effects seen with the systemic treatments. In our previous work, we have shown the ability to extrude plastic filaments with additives, including metal acetates, ceramic, and drugs (gentamicin, methotrexate) with dopant percentages of up to 25% by weight [26]. This method enables complete customization of the dopants added without inhibiting extruder or 3D printer functionality.[26,27]

In the present work, antibacterial 3D printing beads, disks, and filaments were developed using Fused Deposition Modeling (FDM) and our method for creating bioactive filaments.3D printed PMMA doped with gentamicin sulfate, tobramycin, and nitrofurantoin. It was found that through the manufacturing process, these compounds retained their anti-bacterial growth inhibition properties. The results suggest that 3D printed medical devices can be used as a reservoir for localized delivery of a single drug or a suite of drugs and offer the means to provide local therapeutic levels while avoiding systemic toxicity.

2. Materials and methods

2.1. Materials

All plasticware, such as 2 ml Eppendorf tubes, 96 well plates, and pipettes, were purchased from Mid Scientific, St. Louis, MO. For bacterial culture, 100 mm Mueller Hinton agar plates were purchased from Fischer Scientific (Hampton, NH) and *Escherichia coli* ATCC 11775 Vitroids 1000 CFU were from Sigma-Aldrich (St. Louis, MO). *Staphylococcus aureus* was a gift from Dr. Rebecca Girono, Louisiana Tech University. Gentamicin Sulfate (GS), tobramycin and nitrofurantoin were ordered from Sigma-Aldrich (St. Louis, MO). PLA pellets used for extruding filaments were obtained from Push Plastic (Springdale, AR), KJLC 705 silicone oil used for coating pellets was purchased from Kurt J. Lesker Company (Jefferson Hills, PA). Orthoset 3 Radiopaque PMMA bone cement from Wright Medical (Warsaw, IN) was used for 3D printing PMMA bone cements. ExtrusionBot filament extruder was bought from ExtrusionBot, LLC (Phoenix, AZ). MakerBot Replicator 3D printers were purchased form MakerBot (Brooklyn, NY), Nanodrop used for spectrophotometry was from Thermo Scientific (Wilmington, DE), Vulcan A550 Series Benchtop Muffle Furnaces from Thomas Scientific (Swedesboro, NJ) was used for heating biomaterials. OPTA reagent, isopropyl alcohol, and sodium tetraborate were ordered from Sigma-Aldrich (St. Louis, MO). For modeling 3D constructs, Solidworks 2015 was used. For 3D scanning of objects, A Roland Corporation LP-250 desktop 3D scanner (Osaka, Japan) was used.

2.2. Methods

It is critical to understand how 3D printed bioactive constructs compare to current antibacterial implants and in determining the value of this approach. PMMA bone cement is the current gold standard in implant material for the local delivery of antibiotics. All extruded filaments and constructs were tested against comparable commercial grade PMMA materials (used as controls).

2.3. Coating pellets

An oil coating method was used to enable an even dispersion of drugs on the surface of the PLA and PMMA pellets prior to extrusion. KJL 705 silicone oil was chosen to surface coat pellets because of its thermal stability at extrusion temperatures between 170 and 180 °C. The method required a 20 gm batch of pellets, to which was added 15 μL of silicone oil, and pellets were then vortexed to facilitate a uniform coating. These pellets were transferred to another container to avoid loss of drug powder due to adherence of residual oil on the surface of the mixing container. After switching containers, a calculated amount of a drug in powdered form (gentamicin sulfate, nitrofurantoin tobramycin), was added and the pellets were vortexed again.

2.4. Filament extruder

For extruding filaments from coated PLA pellets and PMMA, a first generation ExtrusionBot filament extruder was used. This device operates using a piston-based auger mechanism. Plastic pellets were fed into the hopper at the top of the device. The piston pushes the pellets down to, and through, a metallic die through a heated element. Sensors arranged around this heating element regulate the extrusion temperature. Dies of different diameter at the bottom of the device can be used to customize the thickness of the desired extruded filament.

2.5. Filament extrusion

The MakerBot 1st generation 3D printer used requires a filament diameter of 1.75 mm to print, accordingly, we used a metal die of the same diameter to extrude all filaments. Each 20-gm batch of GS-coated PLA pellets were extruded at 170 °C maintaining the extruded filament diameter at 1.75 mm. We also tried extruding below 170 °C, but that slowed down the extrusion speed and resulted in thicker filaments which were not suitable for 3D printing. At higher temperatures, PLA melted down completely and flowed through the metal die resulting in filaments of uneven diameter.

2.6. Optimization of 3D printing parameters

Preliminary trials revealed that the print-head temperature and filament feed rate have a direct influence on the material flow in

the fabrication of printed constructs. For this reason, optimization of printing parameters for PLA was focused mainly on print-head temperature and filament feed rate. We first determined the minimum temperature of the printer-head required to print PLA and then adjusted the filament extruding rate accordingly. On the MakerBot 1st generation 3D printer, PLA can be printed at the lowest temperature of 215 °C. To compensate for this, we had to decrease the print-head speed from the default of 40 mm/s to 10 mm/s and increase the filament feed rate from a default 18 mm/s to 23 mm/s. The workable range of parameter for a 1.75 mm diameter PLA filament was determined to be a 215 °C printing temperature, 20–23 mm/s of filament feed rate and 12-8 mm/s printer-head speed.

2.7. Scaffold design and fabrication

All 3D CAD models were designed using Solidworks 2015 design software. Solidworks 2015 was used to design all the constructs required for testing the properties of printed scaffolds. All the constructs designed in this CAD program were saved in STL format in order to make these files readily available for the 3D printing.

2.8. Scaffold morphology

For morphological analysis of al constructs, a S4800 Field Emission SEM, HITACHI (Schaumburg, IL) at different magnifications were used. Extruded filaments, 3D printed constructs (discs, beads, and catheters) and controls were all imaged and photodocumented using SEM microscopy.

2.9. Growth inhibition studies-bacterial culture

Bacterial growth inhibition studies were conducted on standard Muller Hinton Agar Plates using *E. coli* and *S. aureus* to assess the bacterial activity of GS. To ensure repeatability, vitroids of these two bacterial strains were used. These viroids were rehydrated and inoculated into agar plates as per the procedures suggested in the manual. Plain PLA pellets, coated PLA pellets, extruded PLA filament, GS loaded PLA filament, beads and constructs were tested. To make sure there was no contamination among agar plates, a blank plate was cultured. An agar plate with just the bacteria acting as the negative control and another with standard GS disc as positive control were also cultured. Under aseptic conditions, samples were inoculated along with the bacteria in the plates and incubated at 37 °C for 24 h. The diameter of inhibition zones was measured at three different points including the samples at the center of the zone and averaged.

2.10. Statistics

All the samples were tested in multiples of 5 for both agar plates and broth cultures. We report all data as mean ± standard deviation (SD). One-way analysis of variance (ANOVA) and the least significant difference (LSD) were used to compare changes among control and experimental groups. A p value of <0.05 was considered statistically significant.

3. Results

3.1. Extruded filaments

The controls and coated pellets were extruded into 1.75 mm diameter 3D printing filaments for fused deposition modeling. An ExtrusionBot filament extruder was used and slight modifications were made to extrude the different filament types as necessary. The extrusion temperature was between the ranges of 170–175 °C. Several meters of each type of filament were extruded. PMMA bone cement filaments were also made to act as comparisons for the PLA ones. This was done by loading the bone cement into a syringe with a tip of similar diameter 1.75 mm diameter.

The filaments were then cut into 1 cm pieces for testing. Small pieces of the filaments were photographed, imaged by SEM and cultured in both plate and broth cultures. It is important to note that controls required filaments to be run on the same plate with the plate divided into quadrants. This led to a need for partial plate images of the quadrants.

3.2. Control filaments

Control PLA filaments were extruded using plain PLA and oil coated PLA pellets using Orthoset® bone cement was mixed and syringe molded into filaments. Photographs and SEM micrographs of the filaments are shown in Fig. 1. PLA filaments had a much smoother surface area and this is likely due to the extrusion temperature with PLA extruded at 170 °C while the polymerization reaction of the PMMA only goes up to 90 °C. Control PLA filaments, oil coated PLA filaments and controlled PMMA filaments were inoculated on bacterial plates as shown in Fig. 2. There was no bacterial zone of inhibition around these control filaments. The filaments were then inoculated in broth cultures as shown in Fig. 3. There was no bacterial inhibition in any of the broth cultures. These control PLA and PMMA standards were used for comparison with all other filaments used in this study.

3.3. Gentamicin filaments

Filaments were fabricated that had 1 wt% or 2.5 wt% gentamicin sulfate by weight. This was done for both extruded PLA and molded PMMA filaments. The filaments were photographed and imaged by SEM as seen in Fig. 4.

The creation of consistent PLA and PMMA filaments that were doped with gentamicin was achieved. It is important to note that care had to be taken with coating oil levels to prevent expansion of the extruded filaments. The 1 wt% and 2.5 wt% gentamicin doped PLA filaments and PMMA filaments were tested on bacterial plates (Fig. 5). Five samples were tested on plates.

The first group of filaments extruded using cleaned extruders and longer purges between extrusions was the 2.5 wt% gentamicin doped PLA (Fig. 5). The average zone of inhibition was 23.13 mm based on two digital caliper measurements. This compared to the 2.5 wt% doped PMMA, which had a zone of inhibition of difference of 22.58 mm Fig. 5B and C. ANOVA analysis showed no difference between these two groups. This differed with the 1 wt% gentamicin doped PLA. Full cleaning purges were not done and resulted in initial filament batches that were either not consistent or were consistent but had too low a level of antibiotic. Only three of the five samples inhibited growth an average 8.52 mm while all handmade PMMA-gentamicin 1 wt% controls inhibited an average of 13.91 mm. This is shown in Fig. 6.

The 1%wt gentamicin doped PMMA had uniformity across all five samples due to hand mixing with mortar and pestle. Greater care could have been taken to clean the extruder and not test filament from the very beginning of a batch. This was done in the further printing of discs and constructs with 1 wt% gentamicin filaments and avoided further issues. The broth cultures for the 1% and 2.5% PLA and PMMA groups are shown in Fig. 7.

The broth cultures showed a consistency of antimicrobial activity of 2.5 wt% gentamicin doped PLA and PMMA. The 1 wt% PLA is only stopping bacterial growth in two out of three broth cultures. This is again noted as the non-consistent mixing of the filament or

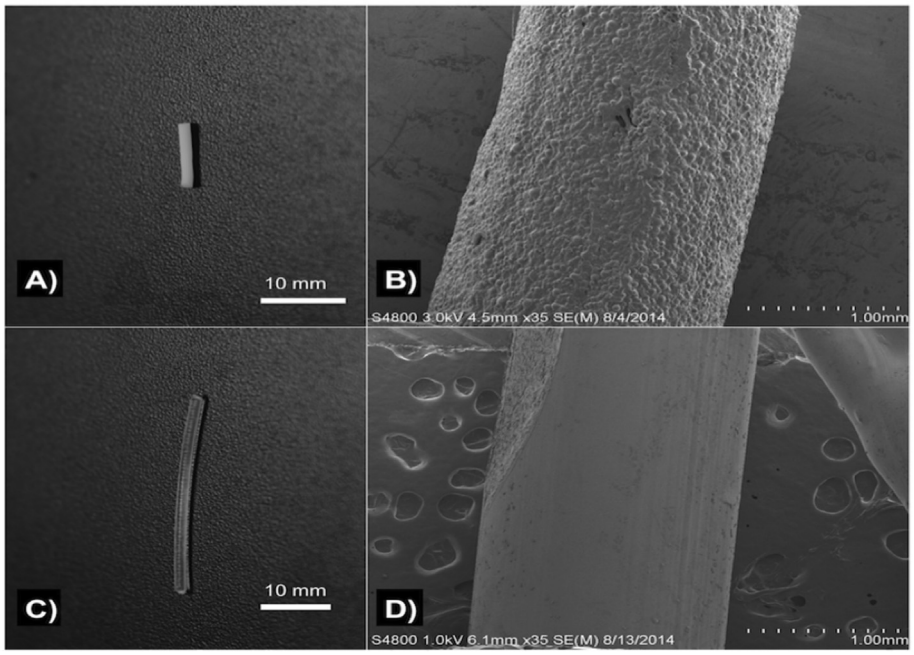

Fig. 1. A) PMMA filament; B) SEM of PMMA filament; C) control PLA filament; D) SEM of control PLA filament.

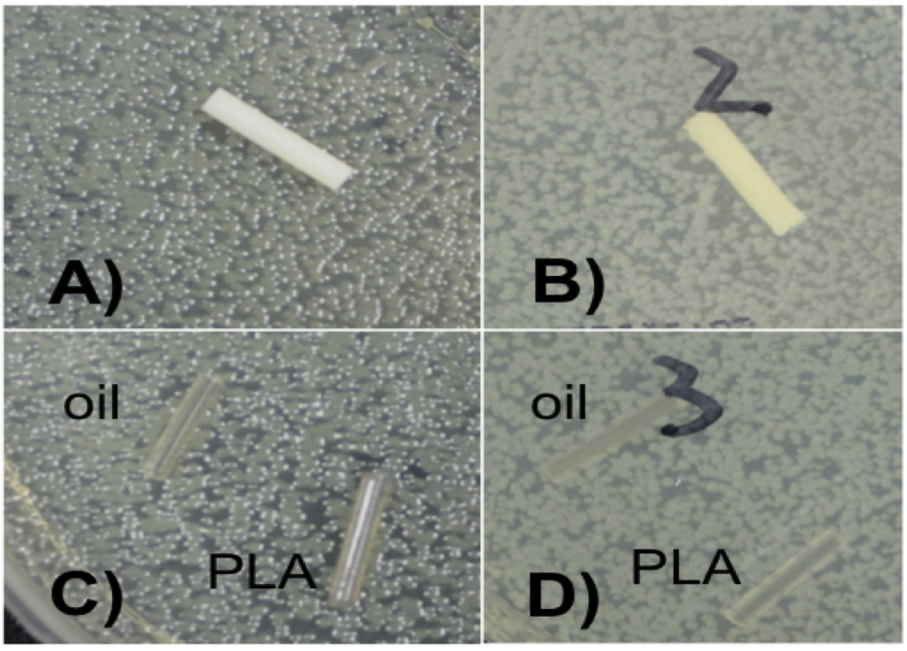

Fig. 2. A) PMMA control top; B) PMMA control bottom; C) PLA and oil coated PLA controls; D) PLA and oil coated PLA controls. *E. coli* = (A, C); *S. aureus* = B, D).

too low a level of antibiotic. There is no growth in the 1 wt% gentamicin doped PMMA. Consistency in the initial extrusion portion from left over material in the auger is a concern and alternative extrusion methods to overcome limitations of the method may need to be developed.

3.4. Tobramycin filaments

Filaments were fabricated that had an addition of 1% or 2.5% tobramycin by weight. It is important to note that while the decomposition point of tobramycin is over 200 °C it melts at 160 °C. The extrusion point was 175 °C. This resulted in a glass or melted sugar like coating occurring. The fabrication was done for both extruded PLA and molded PMMA filaments of the same dopant percentages. The filaments were photographed and imaged by SEM as seen in Fig. 7.

It is important to note that the tobramycin filament is silver in color. The melting of the tobramycin resulted in a color change. Some filament was extruded under the 160 °C and did not exhibit the color change. There is no visible powder in the filament on SEM. The 160 °C filament was not bacterial tested since the printing process would need to be above 200 °C. The filament was tested in

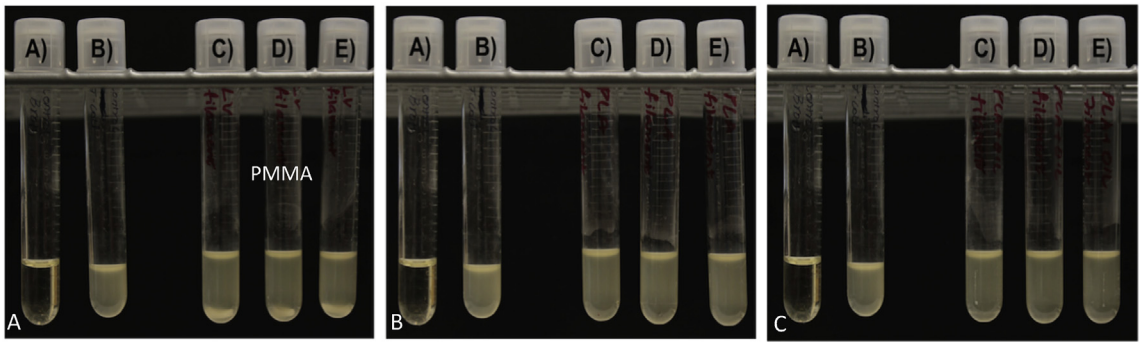

Fig. 3. A. (A) Sterile broth; (B) *E. coli* inoculated broth; C–E) PMMA control filament in broth culture. **B.** (A) Sterile broth B) *E. coli* inoculated broth C–E) Oil coated PLA filament in broth culture. **C.** (A) Sterile broth; (B) *E. coli* inoculated broth; (C–E) Oil coated PLA filament in broth culture.

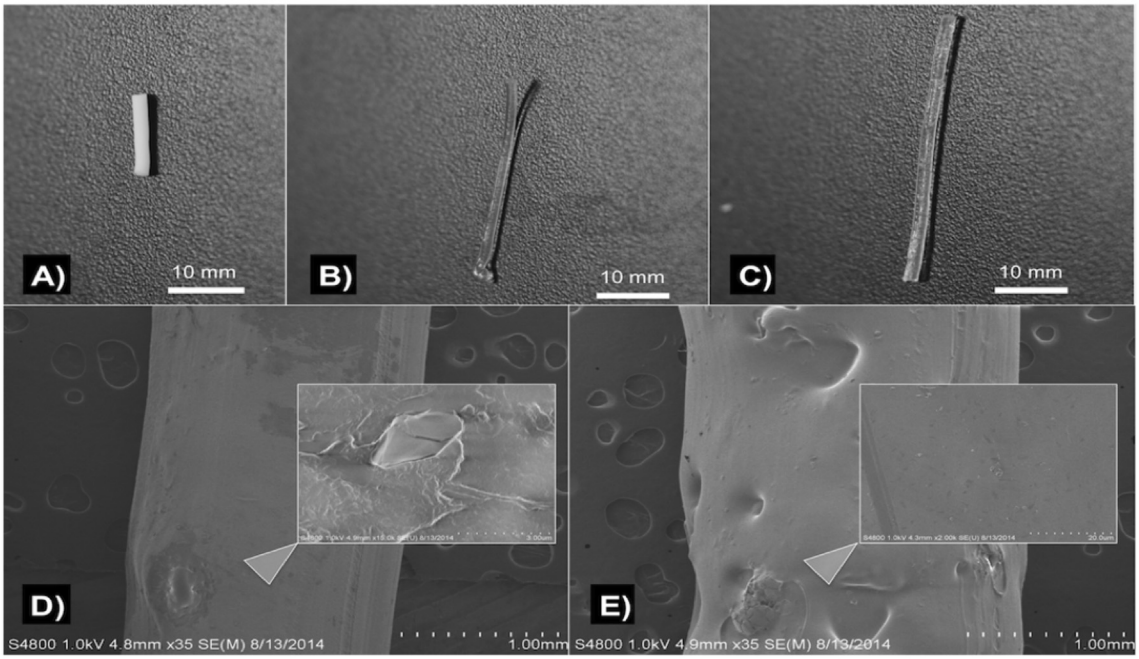

Fig. 4. (A) Gentamicin 1 wt% PMMA filament; (B) Gentamicin 1 wt% PLA filament; (C) gentamicin 2.5 wt% PLA filament; (D) SEM 1% gentamicin 1 wt% PLA filament; (E) SEM gentamicin 5 wt% PLA filament.

order to observe the effect of heating with the PLA bioplastic above the melting point and the kinetics for tobramycin to release. Five Mueller-Hinton plates and three broth cultures were done for 1 cm filaments of PLA mixed with 1.5 wt% tobramycin, 2.5 wt% tobramycin as well as PMMA mixed with 1.5 wt% tobramycin, 2.5 wt% tobramycin.

The tobramycin-PMMA filaments had nearly uniform zones of inhibition within each group (Fig. 8) The 1 wt% tobramycin PMMA zone of inhibition size was 17.17 mm, and the 2.5 wt% tobramycin PMMA zone of inhibition PMMA size was 18.73. This contrasted with the lack of zones of inhibition in the extruded PLA that was mixed with tobramycin. However, it should be noted that some portions of the tobramycin filaments exhibited antimicrobial properties on the plates as shown in Fig. 8. The different effect from gentamicin was likely due to the melting point of tobramycin and possible interaction with the polymer. Similar effects were shown in the broth cultures as shown in Fig. 9.

The PMMA broth cultures had no bacterial growth as was also seen in the PMMA bacterial plate cultures in (Fig. 10). The exothermic PMMA reaction only reaches up to 90 °C so it is below the melting point of tobramycin. The PLA broth cultures for both 1% and 2.5% each only had one broth culture where growth was inhibited (Fig. 9). The PLA extrusion point was above the 160 °C melting point and even placement in a liquid broth did not allow the tobramycin to disperse from the filaments in high enough levels to consistently inhibit bacteria.

3.5. Nitrofurantoin filaments

Filaments were made by extruding nitrofurantoin-coated pellets at a temperature of 175 °C. Nitrofurantoin has a melting point/degradation point more than 240 °C. This was only done for 1 wt% and as a proof of concept since nitrofurantoin has a very low solubility in water. Anti-microbial activity of nitrofurantoin would be viewed as an option for more combinatorial therapy. A construct that combined a highly soluble substance such as gentamicin for an initial burst and also a much more insoluble compound could be desirable. The filament was extruded as shown in Fig. 11A. The yellow nitrofurantoin powder can be seen within the filament. PMMA filament was also made with 1 wt% nitrofurantoin. The

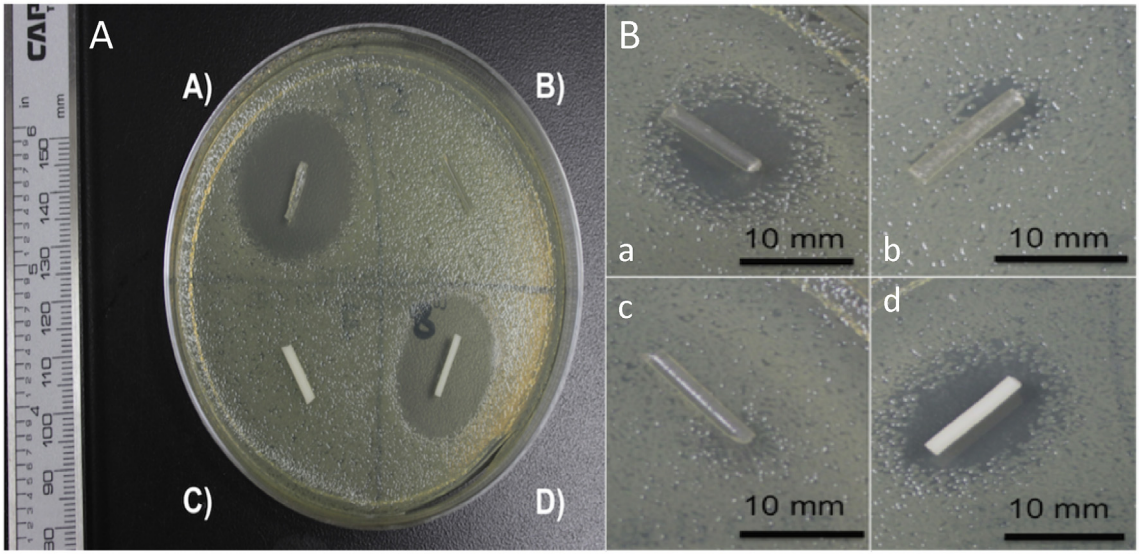

Fig. 5. A. GS doped PLA and PMMA filaments. (A) 2.5 wt% gentamicin PLA filament; (B) Control PLA filament; (C) control PMMA filament; (D) 2.5 wt% gentamicin PMMA filament. **B.** A–C) 1 wt% gentamicin PLA filament D) 1 wt% gentamicin PMMA filament.

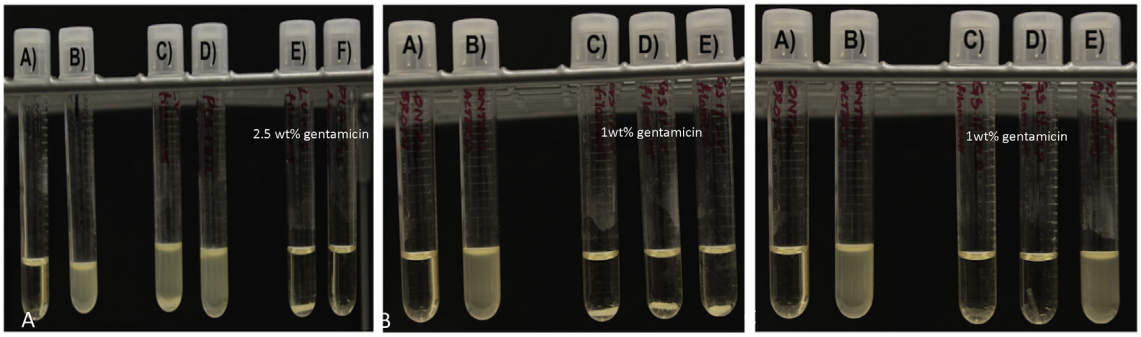

Fig. 6. A. (A) Sterile broth; (B) *E. coli* inoculated broth; (C) Control PMMA; (D) control PLA; (E) 2.5 wt% gentamicin doped PMMA; (F) 2.5 wt% gentamicin doped PLA. **B. (**A) Sterile broth; (B) *E. coli* inoculated broth; (C–E) 1 wt% gentamicin doped PMMA filaments. **6C. (**A) Sterile broth; (B) *E. coli* inoculated broth; (C–E) 1 wt% gentamicin doped PLA filaments.

PMMA filament also had a yellow coloration (Fig. 11B).

Zones of inhibition were photographed and measured on multiple points with a digital caliper. Results for nitrofurantoin plates were inconclusive. All five nitrofurantoin doped PLA filaments had inhibitory properties, but they were quite variable. For example, the zone of inhibition sizes of gentamicin 2.5% wt filament was consistent in size across plates. The zone of inhibition size with the nitrofurantoin filaments was quite variable (Fig. 11B). Three plates had similar partial zone sizes of 5.25 mm. However, of the other two, the largest outlier plate had a zone of 13.5 mm, and the lowest had a 0.5 mm zone of inhibition. This could have been because the doping percent was too low. The gentamicin 1 wt% exhibited similar inconsistencies that were thought to be from improper extrusion. However, the gentamicin powder extruded clear while the nitrofurantoin extruded yellow. It can be seen that there is powder in these filaments. The issue may be inconsistent mixing or too low a doping percentage. This antibiotic also has a very low solubility. Interactions with the polymer chains are not ruled out. PMMA filaments had no antimicrobial properties on the plates.

Broth cultures were also run, and the results are shown in Fig. 12. The broth cultures show no inhibition (1% nitrofuratonin/PLA) or minimal inhibition of bacterial growth (1% nitrofuratonin/PMMA). Only one nitrofurantoin doped PLA filament was able to inhibit growth in the broth culture (Fig. 12A). It seems likely low dopant percentage, low antibiotic solubility, or polymer/antibiotic interaction prevented the desired antimicrobial effect (Fig. 12).

4. Discussion

PMMA is used for the fixation of artificial joints in bone [29] and is extensively used in vertebroplasty [30] and in hip and knee replacement surgery [31,32]. In addition, antibiotic-impregnated PMMA beads, disks, nails and spacers are routinely left in the operative wound to provide a concentration of antibiotics sufficient to kill bacteria while avoiding potential systemic side effects [30,40–44]. Antibiotics are added to PMMA during its creation and many types of antibiotics are used during the mixing process, with gentamicin, tobramycin or vancomycin the most commonly used [30]. Gentamicin and tobramycin are an aminoglycoside antibiotic used to treat various types of bacterial infections, particularly Gram-negative infections. Vancomycin is a glycopeptide antibiotic used in the prophylaxis and treatment of infections caused by Gram-positive bacteria. Vancomycin is a frequently used antibiotic against infections caused by MRSA and is the most commonly used antibiotic worldwide.[25,30] [31] Gentamicin-containing PMMA beads (Septopal®) have been used in Europe for use in treating osteomyelitis since 1970 [33].

In the United States, PMMA has not been accepted by the Food

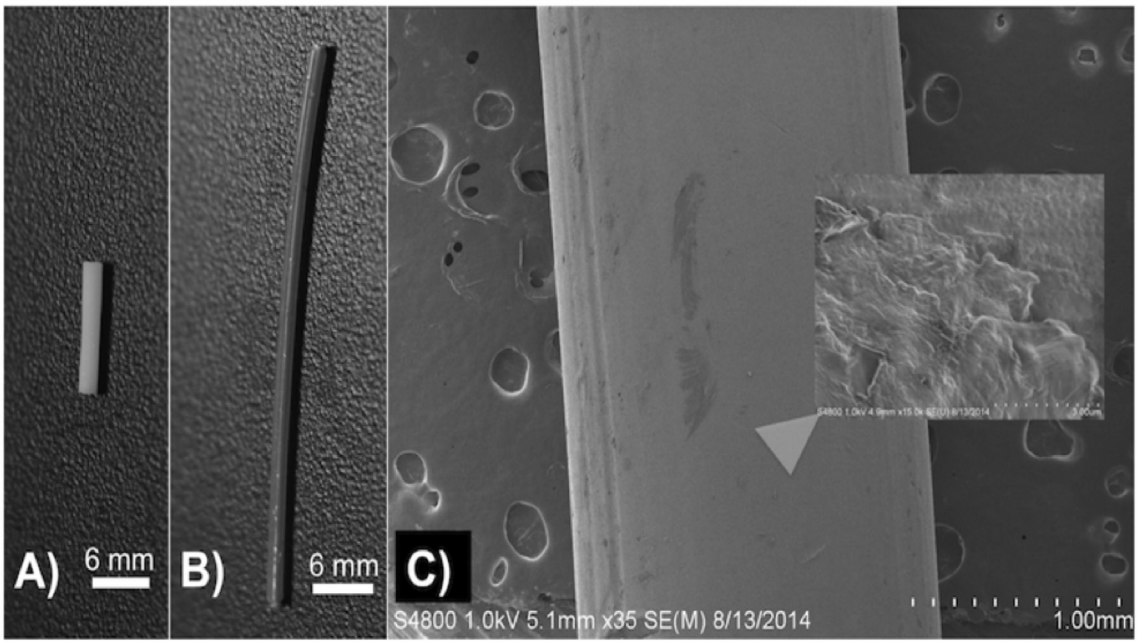

Fig. 7. PLA and PMMA tobramycin doped (1%) filaments. (A) 1 wt% tobramycin doped PMMA; (B) 1 wt% tobramycin doped PLA; (C) SEM 1 wt% tobramycin doped PLA.

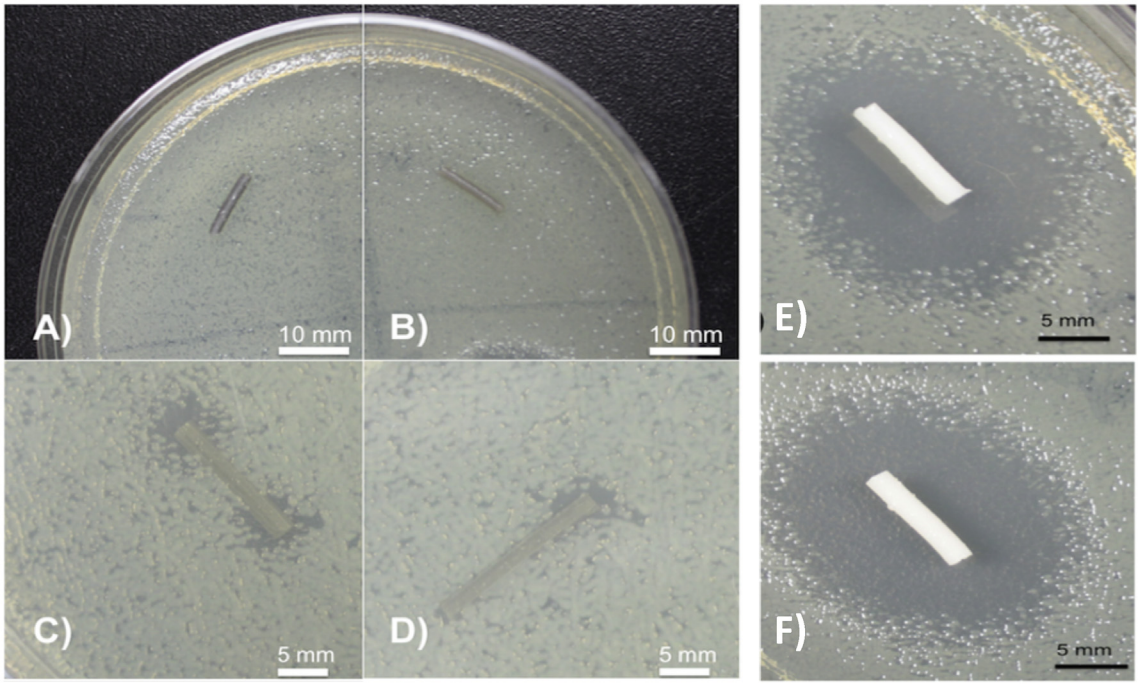

Fig. 8. PLA and PMMA tobramycin doped (1% and 2.5%) filaments. (A) Top 2.5 wt% tobramycin PLA filament; (B) Top 1 wt% tobramycin PLA; (C) Bottom 2.5 wt% tobramycin PLA filament; (D) Bottom 1 wt% tobramycin PLA filament; (E) Top 1% tobramycin PMMA filament; zone of inhibition diameter = 17.17 mm; F) Bottom 2.5% tobramycin PMMA filament, zone of inhibition diameter = 18.83 mm.

and Drug Administration (FDA) requiring surgeons to fabricate their own antibiotic-laced bone cement using commercially available PMMA with an individually made or manufacturer supplied bead mold [29,33,34]. In most procedures, PMMA is mixed with antibiotics by hand, with a mixer, or a sonicator but in all cases, the antibiotics are unevenly distributed throughout the cement [15,22,39]. Furthermore, up to 70% of the antibiotics are released in the first post-operative hours, followed by release at a lower concentration which may be insufficient to prevent biofilm formation with a subsequent increase in treatment failure rates [36–38,40]. The advantages and disadvantages to the use of PMMA-based antibiotic devices in the treatment of osteomyelitis is extensively discussed and highlighted by Barth et al. (2011) [35].

In this study, all antibiotics studied were successfully doped into PMMA and antibiotic-doped PMMA beads, disks, and filaments were effectively printed. The growth inhibition capacity of the antibiotic-loaded PMMA 3D printed constructs was also demonstrated. As each antibiotic-doped PMMA construct is fabricated in a

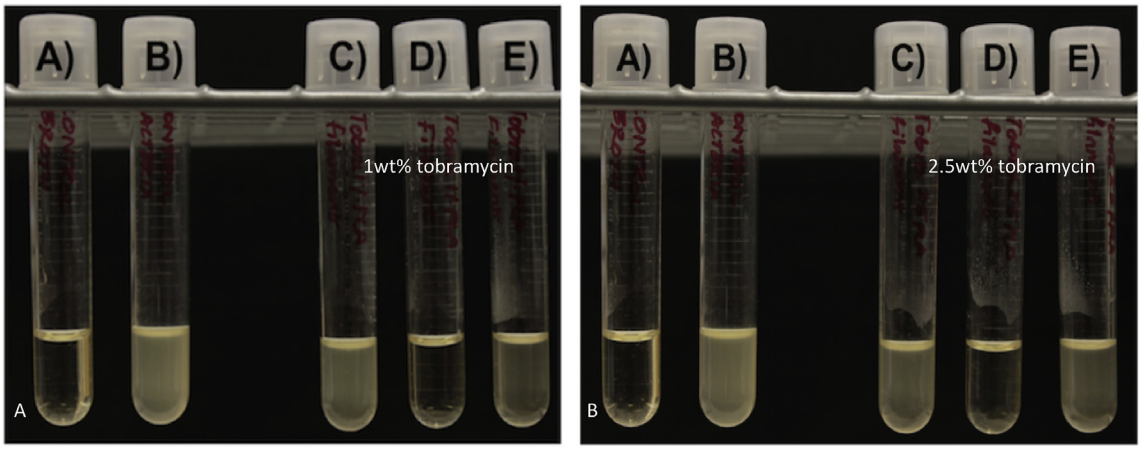

Fig. 9. A. Tobramycin doped PLA filaments. A) Sterile broth; (B) *E. coli* inoculated broth C–E) 1 wt% tobramycin doped PLA filaments. **B.** (A) Sterile broth; (B) *E. coli* inoculated broth; (C–E) 2.5 wt% tobramycin doped PLA filaments.

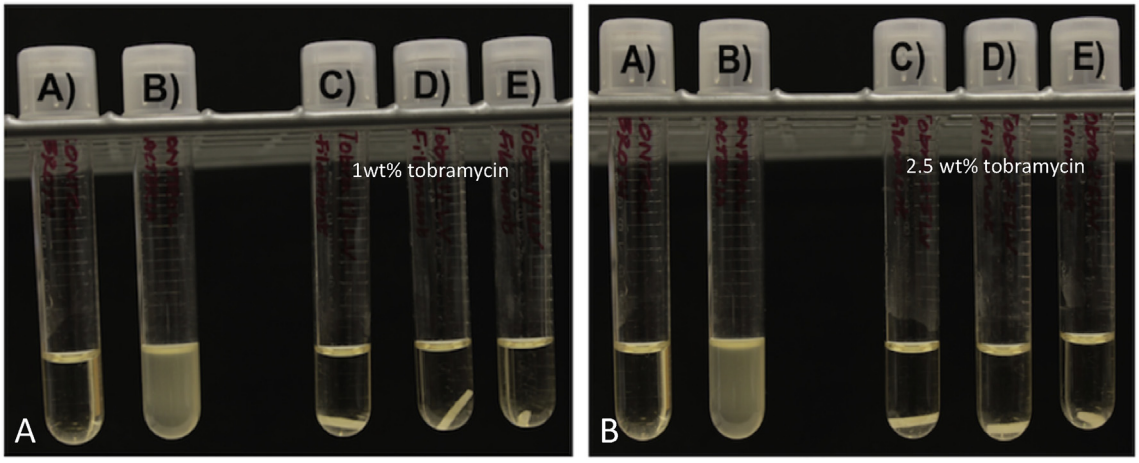

Fig. 10. A. Tobramycin doped PMMA filaments. (A) Sterile broth; (B) *E. coli* inoculated broth; (C–E) 1 wt% tobramycin doped PMMA filaments. **B.** (A) Sterile broth; (B) *E. coli* inoculated broth; (C–E) 2.5 wt% tobramycin doped PMMA filaments.

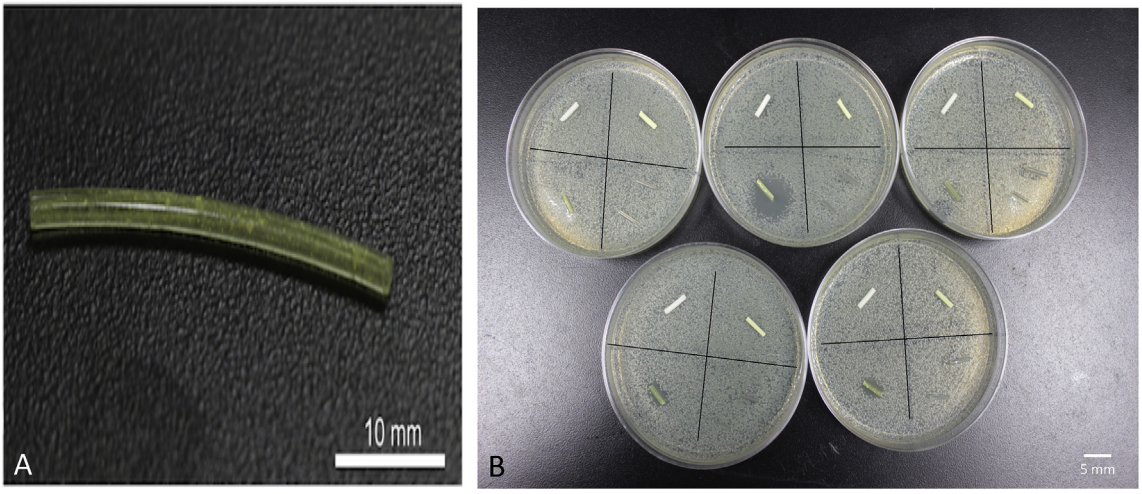

Fig. 11. Nitrofurantoin doped PLA and PMMA filaments. (A) Nitrofurantoin filament. (B) Plates are divided into quadrants with filament with top left being control PMMA, top right being nitrofurantoin 1 wt% PMMA, bottom left nitrofurantoin 1 wt% PLA and bottom right control PLA and oil coated PLA filaments.

layer-by-later fashion this aides in dispersing the antibiotic We employed a computer program to achieve, layer by layer, a pre-designed drug-doped 3D construct [46,47]. This enables the composition of our construct to be varied throughout its structure

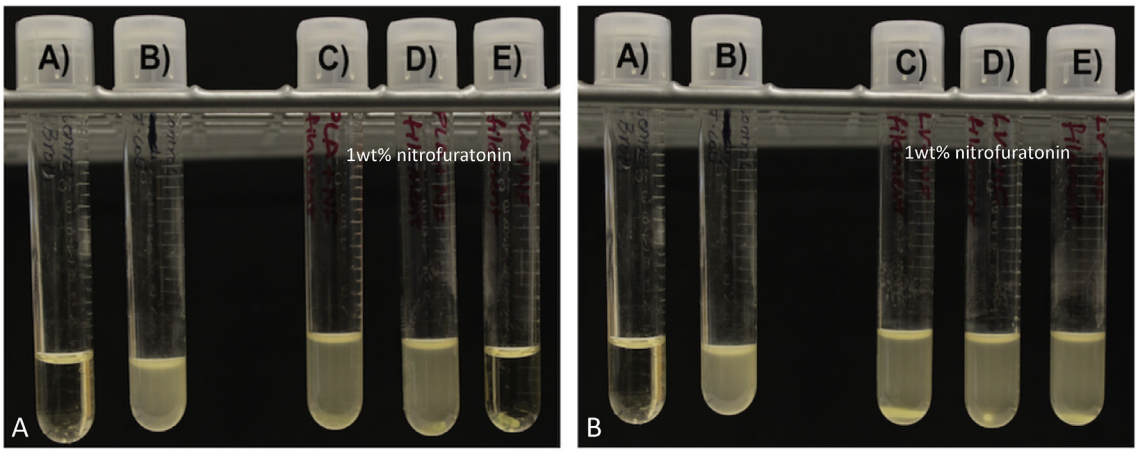

Fig. 12. A. Nitrofurantoin doped PLA filaments. (A) Sterile broth; (B) *E. coli* inoculated broth; (C–E) 1 wt% nitrofurantoin doped PLA filaments. **B. Nitrofurantoin doped PMMA filaments.** (A) Sterile broth; (B) *E. coli* inoculated broth; (C–E) 1 wt% nitrofurantoin doped PMMA filaments.

giving a degree of control lacking in traditional fabrication techniques. Using CAD computer design further offers the opportunity create a more intricate internal architecture that would control the drug release kinetics [47]. CAD design also permits tailored functionality and complexity for patient-specific applications offering personalized medicine to more patients around the world [47]. With multiple print heads, tailored drug delivery systems can be developed that would permit the release of multiple drugs, multiple antibiotic combination or suites of antibiotics and antifungals. Furthermore, strings of beads, layered filaments, disks or any form can be fabricated that contain tailored dosages that target a specific clinical condition or meet the needs of a specific patient treatment. Furthermore, many of the disadvantages with PMMA as discussed above can be eliminated or significantly reduced such as potential tissue necrosis by eliminating the endothermic heat during PMMA polymerization.

Implant-related osteomyelitis (IRO) is a complex bone infection with methicillin-resistant *S. aureus* (MRSA) as the main causative organism [23–25]. Despite new antibiotic regimens, knowledge of the disease, and new material development, peri-prosthetic joint and intramedullary infections are still devastating and a challenging complication in total joint arthroplasty and fracture management with significant impact on our socio-economic system and a patient's life [22,23]. 3D printing technologies offers an opportunity for the manufacture of sophisticated drug delivery systems and biofunctionalized constructs that can specifically target IRO. There are many other advantages to 3D printing antibiotic-doped constructs [44–46]. 3D printing enables the design of simple, cost-effective, drug releasing medical devices that are also patient-specific [26–28,46.47]]. Patient-specific acrylic cranioplasty implants were produced using a low-cost printer [48]. Espalin et al. (2012) fabricated 3D PMMA implants with varying densities and structures for cranial defect repair. Their customized structures were also created with varying porosities using FDM [49]. Finally, fabrication and implantation of three-dimensional craniofacial prototypes, custom-made PMMA implants, and implantation in a small patient population was demonstrated by da Silva et al. (2014) further showing that customized 3D printed PMMA implants are both effective and feasible [50].

5. Conclusions

Local antibiotic delivery systems that deliver high concentrations of antibiotics to the affected site is an area of intense research effort and a pressing great clinical need. We developed a local antibiotic delivery method that addresses wound site and bone infections by providing local release of antibiotics. Furthermore, antibiotics can be delivered singly or in tailored suites directly to the wound site and on the surface of the surgical implants. Gentamicin sulfate, tobramycin, and nitrofurantoin were doped into PMMA and antibiotic-doped 3D printed beads, disks, and filaments were successfully printed. Growth inhibition assays demonstrated the efficacy of antibiotic-loaded PMMA 3D printed constructs in inhibiting bacterial growth.

Conflict of interest

JAW and DKM are co-inventors on the US Patent Application – "Methods and Devices for Three-Dimensional Printing or Additive Manufacturing of Bioactive Medical Devices", Application number US14822275. DKM is the inventor on "Ceramic Nanotube Composite with Sustained Drug Release Capability for Implants, Bone Repair, and Regeneration," United States Patent No. 9,192,912-B1. All other authors claim no conflicts of interest or disclosures.

Acknowledgements

This work was partially funded by the Louisiana Governor's Biotechnology Initiative, The Lagniappe Ladies Fund and a Louisiana Board of Regents Prototype/Proof-of-Concept grant.

References

[1] D. Gomes, M. Pereira, A.F. Bettencourt, Osteomyelitis: an overview of antimicrobial therapy, Braz. J. Pharma. Sci. 49 (1) (2013) 13–17.
[2] L.S. Jorge, A.C. Chueire, A.R. Rossit, Osteomyelitis: a current challenge, Braz. J. Infect. Dis. 14 (3) (2010) 310–315.
[3] I.G. Sia, E.F. Berbari, Osteomyelitis, Best Pract. Res. Clin. Rheumatol. 20 (6) (2006) 1065–1081.
[4] W. Zimmerli, Infection and musculoskeletal conditions: prosthetic-joint associated infections, Best Pract. Res. Clin. Rheumatol. 20 (6) (2006) 1045–1063.
[5] D.P. Lew, F.A. Waldvogel, Osteomyelitis, Lancet 364 (2004) 369–379.
[6] S.K. Nandi, P. Mukharjee, S. Roy, B. Kundu, D. Kumar, D. Basu, Local antibiotic delivery systems for the treatment of osteomyelitis – a review, Mater. Sci. Eng. 29 (2009) 2478–2485.
[7] B. Li, T.J. Webster, Bacteria antibiotic resistance: new challenges and opportunities for implant-associated orthopedic infections, J. Orthop. Res. (2017), https://doi.org/10.1002/jor.23656. Jul 19 [Epub ahead of print].
[8] S.K. Nandi, S. Bandyopadhyay, P. Piyali Das, I. Samanta, P. Mukherjee, S. Roy, B. Kundu, Understanding osteomyelitis and its treatment through local drug delivery system, Biotechnol. Adv. 34 (2016) 1305–1317.
[9] K. Kanellakopoulou, I. Galanopoulos, V. Soranoglou, T. Tsaganos, V. Tziortzioti,

I. Maris, A. Papalois, H. Giamarellou, E.J. Giamarellos-Bourboulis, Treatment of experimental osteomyelitis caused by methicillin-resistant Staphylococcus aureus with a synthetic Carrier of calcium sulphate (Stimulan®) releasing moxifloxacin, Int. J. Antimicrob. Agents 33 (4) (2009) 354–359.
[10] X. Zhang, W. Jia, Y. Gu, W. Xiao, X. Liu, D. Wang, C. Zhang, W. Huang, M.N. Rahaman, D.E. Day, Teicoplanin-loaded borate bioactive glass implants for treating chronic bone infection in a rabbit tibia osteomyelitis model, Biomaterials 31 (22) (2010) 5865–5874.
[11] K. Anagnostakos, J. Kelm, T. Regitz, et al., In vitro evaluation of antibiotic release from and bacteria growth inhibition by antibiotic-loaded acrylic bone cement spacers, J. Biomed. Mater. Res. Part B Appl. Biomater. 72 B (2005) 373–378.
[12] R. Thonse, J.D. Conway, Antibiotic cement-coated nails for the treatment of infected nonunions and segmental bone defects, J. Bone Jt. Surg. Am. 90 (2008) 163–174.
[13] A.K. Bhadra, C.S. Roberts, Indications for antibiotic cement nails, J. Orthop. Trauma 23 (2009) S26–S30.
[14] M. Sukeik, F.S. Haddad, Two-stage procedure in the treatment of late chronic hip infections-spacer implantation, Int. J. Med. Sci. 6 (2009) 253–257.
[15] M.E. Hake, H. Young, D.J. Hak, P.F. Stahel, E.M. Hammerberg, C. Mauffrey, Local antibiotic therapy strategies in orthopaedic trauma: practical tips and tricks and review of the literature, Injury 46 (8) (2011) 1447–1456.
[16] N.C. Lindfors, P. Hyvönen, M. Nyyssönen, M. Kirjavainen, J. Kankare, E. Gullichsen, J. Salo, Bioactive glass S53P4 as bone graft substitute in treatment of osteomyelitis, Bone 47 (2010) 212–218.
[17] T.J. Mäkinen, M. Veiranto, P. Lankinen, N. Moritz, J. Jalava, P. Törmälä, H.T. Aro, In vitro and in vivo release of ciprofloxacin from osteoconductive bone defect filler, J. Antimicrob. Chemother. 56 (2005) 1063–1068.
[18] Z. Xie, X. Liu, W. Jia, C. Zhang, W. Huang, J. Wang, Treatment of osteomyelitis and repair of bone defect by degradable bioactive borate glass releasing vancomycin, J. Contr. Release 139 (2009) 118–126.
[19] C.L. Romanò, N. Logoluso, E. Meani, D. Romanò, E. De Vecchi, C. Vassena, L. Drago, A comparative study of the use of bioactive glass S53P4 and antibiotic-loaded calcium-based bone substitutes in the treatment of chronic osteomyelitis: a retrospective comparative study, Bone Jt. J. 96 (6) (2014) 845–850.
[20] F. Lalidou, G. Kolios, G.I. Drosos, Bone infections and bone graft substitutes for local antibiotic therapy, Surg. Technol. Int. 24 (2014) 353–362.
[21] T. Fang, J. Wen, J. Zhou, Z. Shao, J. Dong, Poly (ε-caprolactone) coating delays vancomycin delivery from porous chitosan/β-tricalcium phosphate composites, J. Biomed. Mater. Res. B Appl. Biomater. 100 (7) (2012) 1803–1811.
[22] M. Zilberman, J.J. Elsner, Antibiotic-eluting medical devices for various applications, J. Contr. Release 130 (2008) 202–215.
[23] G. Schmidmaier, M. Lucke, B. Wildemann, et al., Prophylaxis and treatment of implant-related infections by antibiotic-coated implants: a review, Injury 37 (2006) S105–S112.
[24] Z. Orhan, E. Cevher, A. Yıldız, R. Ahıskalı, D. Sensoy, L. Mülazımoğlu, Biodegradable microspherical implants containing teicoplanin for the treatment of methicillin-resistant Staphylococcus aureus osteomyelitis, Arch. Orthop. Trauma Surg. 130 (2010) 135–142.
[25] J.L. Jiang, Y.F. Li, T.L. Fang, J. Zhou, X.L. Li, Y.C. Wang, J. Dong, Vancomycin-loaded nano-hydroxyapatite pellets to treat MRSA-induced chronic osteomyelitis with bone defect in rabbits, Inflamm. Res. 61 (2012) 207–215.
[26] J. Weisman, N. Kaskas, A.H. Green, D. Ballard, J.J. Ambrose, L. Sun, D.K. Mills, Three-dimensional printing of chemotherapeutic and antibiotic eluting fibers, seeds, and discs for localized drug delivery in cutaneous disease, J. Invest. Dermatol. 135 (2015) S87–S98.
[27] D.H. Ballard, J.A. Weisman, U. Jammalamadaka, K. Tappa, S. Alexander, F. Griffen, Three-dimensional printing of bioactive hernia meshes: in vitro proof of principle, Surgery (2017), https://doi.org/10.1016/j.surg.2016.08.033, 2016 Oct 7. pii: S0039–6060(16)30467-6 [Epub ahead of print].
[28] J. Weisman, N. Kaskas, A.H. Green, D. Ballard, J.J. Ambrose, L. Sun, D.K. Mills, Three-dimensional printing of chemotherapeutic and antibiotic eluting fibers, seeds, and discs for localized drug delivery in cutaneous disease, J. Invest. Dermatol. 135 (2015) S87–S98.
[29] L. Alvarez, M. Alcaraz, A. Pérez-Higueras, J.J. Granizo, I. de Miguel, R.E. Rossi, D. Quinones, Percutaneous vertebroplasty: functional improvement in patients with osteoporotic compression fractures, Spine 31 (2006) 1113–1118.
[30] J.C.J. Webb, R.F. Spencer, The role of polymethylmethacrylate bone cement in modern orthopaedic surgery, J. Bone Jt. Surg. Br. 89 (2007) 851–857.
[31] K.-D. Kühn, Properties of bone cement: what is bone cement, in: S. Breusch, H. Malchau (Eds.), The Well-Cemented Total Hip Arthroplasty, Springer Medizin Verlag, Heidelberg, 2005, pp. 52–59.
[32] G.H. Heyse-Moore, R.S.M. Ling, Current cement techniques, in: Progress in Cemented Total Hip Surgery and Revision, Symposium, Amsterdam, 1982, pp. 71–86.
[33] G.H.I.M. Walenkamp, Self-mixed antibiotic bone cement: western countries learn from developing countries, Acta Orthop. 80 (2009) 505–507.
[34] P.D. Holtom, M. Patzakis, Newer methods of antimicrobial delivery for bone and joint infections, Instr. Course Lect. 52 (2003) 745–749.
[35] T. Jaeblon, Polymethylmethacrylate: properties and contemporary uses in orthopaedics, J. Am. Acad. Orthop. Surg. 18 (2010) 297–305.
[36] M. Virto, P. Frutos, S. Torrado, G. Frutos, Gentamicin release from modified acrylic bone cements with lactose and hydroxypropylmethylcellulose, Biomaterials 24 (2003) 79–87.
[37] H. van de Belt, D. Neut, W. Schenk, J. van Horn, H. van der Mei, H. Busscher, Gentamicin release from polymethylmethacrylate bone cements and *Staphylococcus aureus* biofilm formation, Acta Orthop. Scand. 71 (6) (2000) 625–629.
[38] C. Ragel, M. Vallet-Regi, In vitro bioactivity and gentamicin release from glass-polymer-antibiotic composites, J. Biomed. Mater. Res. A 51 (3) (2000) 424–429.
[39] M.L. Azi, M.K. Junior, R. Martinez, C.A. Paccola, Bone cement and gentamicin in the treatment of bone infection: background and in vitro study, Acta Ortop. Bras. 18 (1) (2010) 31–34.
[40] N.J. Dunne, J. Hill, P. McAfee, R. Kirkpatrick, S. Patrick, M. Tunney, Incorporation of large amounts of gentamicin sulphate into acrylic bone cement: effect on handling and mechanical properties, antibiotic release, and biofilm formation, Proc. Inst. Mech. Eng. H 222 (2008) 355–365.
[41] K. Anangnostakos, O. Furst, J. Kelm, Antibiotic-impregnated PMMA hip spacers. Current status, Acta Orthop. 77 (2006) 628–637.
[42] K. Anagnostakos, J. Kelm, T. Regitz, et al., In vitro evaluation of antibiotic release from and bacteria growth inhibition by antibiotic-loaded acrylic bone cement spacers, J. Biomed. Mater. Res. Part B Appl. Biomater. 72B (2005) 373–378.
[43] R. Thonse, J.D. Conway, Antibiotic cement-coated nails for the treatment of infected nonunions and segmental bone defects, J. Bone Jt. Surg. Am. 90 (2008) 163–174.
[44] J.A. Inzana, R.P. Trombette, E.M. Schwartz, S.L. Kates, H.A. Awad, 3D printed bioceramics for dual antibiotic delivery to treat implant-associated bone infection, Eur. Cells Mater. 30 (2015) 232–247.
[45] J.A. Lewis, G.M. Gratson, Direct writing in three dimensions, Mater. Today 7 (2004) 32–39.
[46] S.E. Moulton, G.G. Wallace, 3-dimensional (3D) fabricated polymer based drug delivery systems, J. Contr. Release (2014) 19327–19334.
[47] S. Sandler, M. Preis, Printed drug-delivery systems for improved patient treatment, Trends Pharm. Sci. 37 (2016) 1070–1080.
[48] E.T.W. Tan, J.M. Ji Min Ling, S.K. Dinesh, The feasibility of producing patient-specific acrylic cranioplasty implants with a low-cost 3D printer, J. Neurosurg. 124 (2016) 1531–1537.
[49] D. Espalin, K. Arcaute, D. Rodriguez, F. Medina, M. Posner, D. Wicker, Fused deposition modeling of polymethylmethacrylate for use in patient-specific reconstructive surgery, Rap Proto 16 (3) (2010) 164–173.
[50] A.L. Fernandes da Silva, A.M. Borba, N.R. Simão, F.L.M. Pedro, A.H. Borges, M. Miloro, Customized polymethyl methacrylate implants for the reconstruction of craniofacial osseous defects, Case Rep. Surg. (2014), 358569, https://doi.org/10.1155/2014/358569.